Block copolymer multiple patterning integrated with conventional ArF lithography†

Seung Hak Park,[a] Dong Ok Shin,[a] Bong Hoon Kim,[a] Dong Ki Yoon,[b] Kyoungseon Kim,[b] Si Yong Lee,[b] Seok-Hwan Oh,[b] Seong-Woon Choi,[b] Sang Chul Jeon[c] and Sang Ouk Kim*[a]

Received 13th July 2009, Accepted 24th August 2009
First published as an Advance Article on the web 17th September 2009
DOI: 10.1039/b913853f

We present block copolymer multiple patterning as an efficient and truly scalable nanolithography for sub-20 nm scale patterning, synergistically integrated with conventional ArF lithography. The directed assembly of block copolymers on chemically patterned substrates prepared by ArF lithography generated linear vertical cylinder arrays with a 20 to 30 nm diameter, enhancing the pattern density of the underlying chemical patterns by a factor of two or three. This self-assembled resolution enhancement technique affords a straightforward route to highly ordered sub-20 nm scale features *via* conventional lithography.

Introduction

Photolithography is a key enabling technology that has served for the continuous miniaturization of semiconductor devices. The successful scaling down of photolithography for sub-30 nm scale patterning is an urgent and decisive requirement for creating novel nanodevices as well as next generation CMOS technology.[1,2] However, conventional projection photolithography, established upon the simple principle of mask-through radiation of photosensitive materials, is close to its intrinsic resolution limit defined by optical scattering and the complexity of illuminating systems.

Double patterning is a promising resolution enhancement technique widely used in conjunction with conventional photolithography. Multiple cycles of overlaid exposing and etching steps may generate a pattern whose minimum pattern resolution reaches half of the optical resolution limit (see Fig. 1a).[3–5] Several approaches such as self-aligned double patterning and positive/negative tone double patterning have been exploited such that the pattern resolution of conventional photolithography could be enhanced without any high energy beam source or high refractive index fluid immersion. Nevertheless, these approaches involving multiple exposing steps are highly sensitive to overlay errors between multiple exposures and require complex mask design and highly sensitive photoresists.[6,7]

We developed block copolymer multiple patterning, which can produce sub-20 nm scale dimensions *via* a single exposure step, synergistically combining conventional 193 nm ArF projection photolithography with block copolymer self-assembly. Block copolymers are self-assembling polymeric materials consisting of covalently linked, immiscible macromolecular blocks. The microphase separation of immiscible macromolecular blocks results in spontaneous assembly into periodic arrays of nanoscale spheres, cylinders, or lamellae whose characteristic dimensions are tunable in the range 3–50 nm.[8,9] Block copolymer lithography utilizes the nanoscale self-assembled morphology of block copolymer thin films as templates for nanofabrication.[10–24] Recently, block copolymer lithography was used in air-gap technology for semiconductor devices, where the vacuum gap generated by means of the block copolymer nanoporous template remarkably relieves the interference between neighboring conducting wires.[25,26] For further progress of block copolymer lithography towards laterally ordered, addressable nanopatterning, the integration of block copolymer assembly with a pre-existing lithographic process is highly demanded.[12–15]

In this work, we employed block copolymer lithography to enhance the pattern density of conventional 193 nm ArF projection photolithography, which is currently used in the mass-production of commercial semiconductor devices and anticipated to serve for device fabrication for a while due to the technological barriers for the development of illumination systems using shorter wavelength light sources such as EUV (λ = 13.5 nm). In our approach, unlike conventional photolithography which produces a topographic photoresist pattern, a stripe surface pattern having periodic variation of surface chemistry is produced by ArF lithography. Owing to the modulated interfacial tension of the surface pattern towards the chemically heterogeneous self-assembled morphology, directed assembly of asymmetric block copolymer blend films upon the surface chemical pattern (pattern pitch, L_s: 143 nm) generated highly-ordered, multiple arrays of self-assembled cylinders with a layer pitch (L_l) of 30 to 60 nm, which enhanced the surface pattern density prepared by ArF photolithography by a factor of two or three. This approach, requiring only a single exposure and no intermediate etching, is highly compatible to continuous device processing and greatly diminishes the burden for overlay

[a]*Department of Materials Science and Engineering, KAIST, Daejeon, 305-701, Republic of Korea. E-mail: sangouk.kim@kaist.ac.kr; Fax: +82 42 350 3310; Tel: +82 42 350 3339*
[b]*Semiconductor R&D Center, Device Solution Division, Samsung Electronics San #16, Banwol-Dong, Hwasung City, Gyeonggi-Do 445-701, Republic of Korea*
[c]*National Nanofab Center, 373-1, Guseong-dong, Yuseong-gu, Daejeon 305-701, Republic of Korea*
† Electronic Supplementary Information (ESI) available: Fig. S1–S3. See DOI: 10.1039/b913853f/

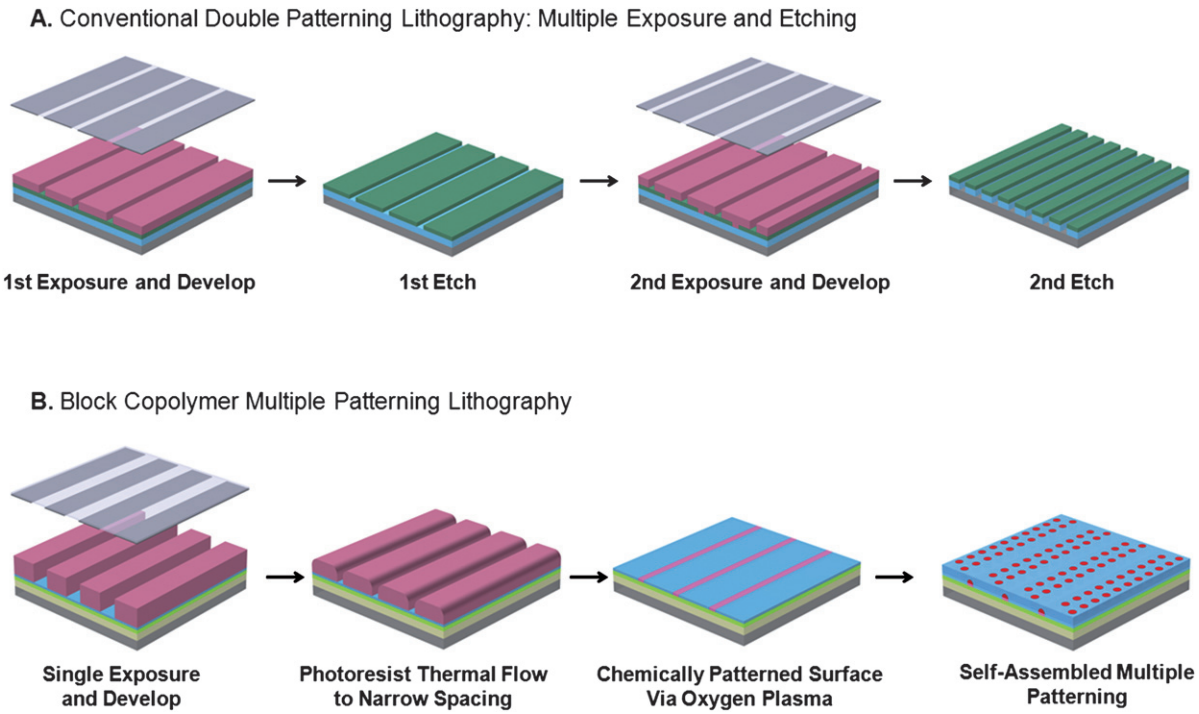

Fig. 1 Schematic description contrasting the conventional double patterning lithography with the block copolymer multiple patterning lithography. (a) Conventional double patterning requires multiple cycles of exposing and etching steps. (b) Block copolymer multiple patterning requires only a single exposure step and no intermediate etching step. Directed block copolymer assembly into multiple cylinder arrays enhances the pattern density of the surface chemical pattern prepared by conventional ArF lithography by a factor of two or three.

control and complex mask design. Most significantly, this approach successfully overcomes the intrinsic optical resolution limit of conventional photolithography by combining with self-assembling materials. While the state-of-art mass-producible photolithographic process employing immersion lithography can achieve the pattern pitches of 78 nm scale for line-and-space pattern and 115 nm for contact holes, our block copolymer multiple patterning routinely generates linearly arrayed sub-20 nm scale nanoholes or nanopillars.

Experimental

Materials

Polished 8 in. diameter silicon wafers were obtained from SUMCO. All block copolymers used in this study were purchased from Polymer Source, Inc. Hydroxyl-terminated random copolymer (PS-*r*-PMMA) with a narrow molecular weight distribution was prepared by a living free-radical polymerization. Tetraethylammonium hydroxide (TEAH), anhydrous toluene and cyclohexanone were purchased from Aldrich and used as received. Chemicals for a 'spin-on carbon' layer and 'spin-on silicon' layer were obtained from Nissan chemicals and ShinEtsu chemicals, respectively. Deionized water (18 MΩ) was used throughout the experiments.

Preparation of an ARC coated silicon substrate

A 200 nm thick spin-on carbon (SOC) layer was spin cast on a silicon wafer and baked at 250 °C for 1 min. An 80 nm thick spin-on silicon anti-reflective coating layer (Si-ARC) was spin cast on the SOC layer and baked at 250 °C for 1 min for curing. The prepared trilayered substrate was immersed in an aqueous solution of tetraethylammonium hydroxide (0.5 wt%) for 30 min to incorporate reactive hydroxyl functional groups at the surface of the Si-ARC layer. After sufficient cleaning with deionized water, the wafer was dried under a dry N_2 stream.

Formation of the polymer brush imaging layer

A thin layer of end-functionalized random copolymer, hydroxyl-terminated PS-*r*-PMMA (M_w = 40 kg/mol, 58 vol% styrene, 42 vol% methy methacrylate, PDI = 1.9) was spin coated on the surface functionalized trilayered substrate from a toluene solution. A monolayer brush of the random copolymer was covalently linked to the substrate surface by vacuum annealing at 160 °C for 72 h. The ungrafted brush layer was spin-washed by toluene.

Chemical prepatterning *via* ArF photolithography

A 160 nm thick photoresist (ShinEtsu) for an ArF wavelength (193 nm) was spin coated on the surface of the polymer brush imaging layer. Soft bake (110 °C) was applied to remove residual solvents and densify the photoresist layer. A Nikon S-308 ArF scanner equipped with a photomask having a 1:1 line-and-space (L/S) ratio and pattern pitch of 143 nm was used for exposure. After exposure and subsequent development, the patterned wafer was dried at 100 °C for 1 min. The SEM measurements of the patterns revealed a 1:1 L/S ratio with a 143 nm pattern pitch. The L/S ratio was further tuned to 3:1 by thermal flow of photoresist

performed at 150 °C for 40 s. The asymmetrically L/S patterned wafer was placed in an O_2 plasma chamber for 20 s to induce selective oxidation of the brush layer exposed to air in the narrow space of the photoresist pattern. After plasma treatment, the remaining photoresist was completely washed to leave a highly asymmetric chemical pattern consisting of alternating wide neutral and narrow polar stripes.

Pattern density enhancement by directed block copolymer assembly

Binary blends of cylinder-forming diblock copolymers (PS-*b*-PMMA1; M_n of PS block: 46.1 kg/mol, M_n of PMMA block: 21 kg/mol, PDI = 1.08 and PS-*b*-PMMA2; M_n of PS block: 140 kg/mol, M_n of PMMA block: 60 kg/mol, PDI = 1.09) were prepared by solution mixing in toluene. The pattern period of the hexagonal packed cylinder morphology of block copolymer blends was tuned by blend composition. A 20 nm thick binary blend thin film was spin-coated on the chemically patterned surface from toluene solution and annealed at 190 °C to induce directed assembly.

Pattern transfer into a metal nanodot array and silica nanopillar array

A multiple patterned block copolymer thin film was exposed to a UV radiation to selectively degrade PMMA cylinders and crosslink the PS matrix. The degraded PMMA cylinders were completely cleaned by O_2 RIE. The remaining crosslinked nanoporous PS layer was used as a deposition mask. A 10 nm thick Al film was selectively deposited through a PS nanotemplate, which was subsequently lifted-off by sonication. A well-ordered Al nanodot array precisely replicating the block copolymer multiple patterned morphology was produced over a large area The metal nanodot array was used as the etching mask for CF_4 RIE of the underlying ARC layer. Silica pillar arrays were created by RIE over a large area.

Results and discussion

We used the binary blends of two asymmetric poly(styrene-*block*-methyl methacrylate) copolymers (PS-*b*-PMMA1; M_n of PS block: 46.1 kg/mol, M_n of PMMA block: 21 kg/mol and PS-*b*-PMMA2; M_n of PS block: 140 kg/mol, M_n of PMMA block: 60 kg/mol) forming the hexagonally packed PMMA cylinder in the PS matrix as self-assembling polymers. As summarized in Table 1, the cylinder layer spacing (L_l) varied from 30.9 nm to 60.6 nm with blend composition (f) (see ESI†, Fig. S1). Fig. 1b schematically describes the block copolymer multiple patterning procedure. A photoresist layer was spin-coated upon a substrate surface neutrally modified with a random copolymer brush (polystyrene-*random*-poly(methyl methacrylate); PS-*r*-PMMA) layer.[27] A single exposure step using ArF projection photolithography and the following thermal flow process generated the line-and-space pattern of a photoresist whose pattern pitch was 143 nm and line width and spacing (L/S) ratio was highly asymmetric (approximately 3:1). An oxygen plasma treatment over the entire substrate surface selectively oxidized the polymer brush layer exposed in the narrow space region of the photoresist pattern.[28] After solvent washing of the photoresist, a highly asymmetric chemical pattern consisting of an alternating wide (~105 nm) neutral stripe and a narrow (~35 nm) oxidized polar stripe remains on the substrate surface, replicating the topographic pattern of the photoresist. A thin film of block copolymer blends was spin-coated upon the asymmetric chemical pattern and thermally annealed. Multiple arrays of vertical cylinders were spontaneously assembled along the underlying stripe pattern, greatly enhancing the pattern density of the lithographically defined underlying chemical pattern.

A crucial requirement for successful block copolymer multiple patterning is the preparation of a well-defined substrate prepattern with a highly asymmetric L/S ratio. We accomplished this task by means of conventional ArF Lithography. Unlike high energy light sources such as EUV or E-beam which can generate an ultrafine nanopattern in the photoresist layer on

Table 1 Characteristic dimensions for the self-assembled nanoscale morphologies of asymmetric PS-*b*-PMMA block copolymer blend films[a]

f	L_c (nm)	L_l (nm)	L_s/L_l	Morphology
0	35.7	30.9	4.62	
0.2	**42**	**36.3**	3.93	Fig. 3c
0.4	48.8	42.2	3.38	
0.5	**53.4**	**46.2**	3.09	Fig. 3b
0.6	56.9	49.2	2.9	
0.8	63	54.5	2.62	
1	**70**	**60.6**	2.35	Fig. 3a

[a] f: Weight fraction of PS-*b*-PMMA2 in the binary blends of PS-*b*-PMMA1 and PS-*b*-PMMA2, L_c: center to center distance between neighboring cylinders of a blend film, L_l: cylinder layer spacing of a blend film, L_s: surface chemical pattern pitch, 143 nm .

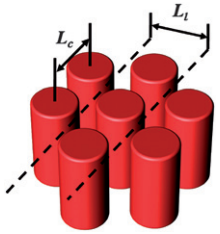

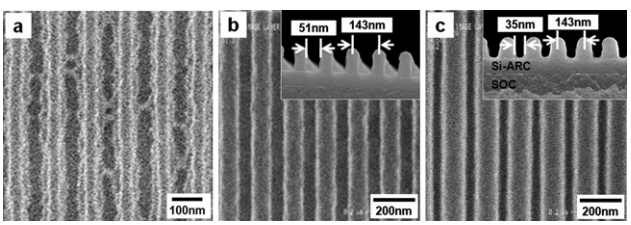

Fig. 2 A series of SEM images of the photoresist pattern created by conventional ArF lithography and subsequent thermal flow. (a) Plain view of a photoresist pattern with poor line edge roughness, prepared without an anti-reflective coating (ARC) layer in the underlying substrate. (b) Plain and cross-sectional (inset) views of a symmetric photoresist pattern prepared with an ARC layer. A 200 nm thick spin-on-carbon (SOC) layer and an 80 nm thick silsesquioxane based ARC (Si-ARC) layer were deposited on the underlying silicon substrate. (c) Plain view and cross-sectional (inset) of a highly asymmetric photoresist pattern whose line/spacing ratio was tuned by a thermal flow process.

a bare Si substrate, an ArF excimer laser having a long wavelength of 193 nm requires an antireflective coating (ARC) layer to prevent pattern distortion due to beam reflection at the Si surface. Fig. 2a presents the plane view of a photoresist pattern with a poor line edge roughness generated by ArF lithography without an ARC layer. Upon exposure to an ArF excimer laser, the beam reflected at the Si surface and interfered with the incoming beam to generate the intensity profile, resulting in a poor line edge of the photoresist pattern. In order to enhance the pattern fidelity, a 200 nm thick spin-on-carbon (SOC) layer and an 80 nm thick silesquioxane based anti-reflective coating (Si-ARC) layer were sequentially stacked on a silicon substrate (Fig. 2b). This trilayered substrate is widely used in the mass-production of a commercial semiconductor device.[29]

The surface of the Si-ARC layer was covalently modified with a neutral PS-*r*-PMMA brush layer that played a role of an imaging layer for chemical patterning. This neutral brush layer had an identical interfacial tension to PS and PMMA components such that thin film confinement induced surface perpendicular cylinder morphology in PS-*b*-PMMA copolymer blend films.[27] Furthermore, this layer could be selectively oxidized by a lithographic process to constitute a surface pattern with alternating neutral and oxidized polar (PMMA preferential) stripes. Owing to the Si-ARC layer, a symmetric (1:1 L/S ratio) stripe pattern of a photoresist with the pattern period of 143 nm could be successfully prepared on a brush-treated substrate surface, exactly replicating a photomask pattern. The symmetric photoresist pattern was transformed into a highly asymmetric line-and-space pattern by a thermal flow process performed at 150 °C for 40 s (Fig. 2c). This L/S ratio tuning method, which relies upon the thermoplastic deformation of a polymeric photoresist at an elevated temperature, is widely utilized in the commercial device manufacturing process for a narrow contact hole or narrow space formation.[30] The asymmetric topographic pattern of the photoresist was replicated into a chemical pattern of the underlying polymer brush imaging layer by selective O_2 reactive ion etching (RIE).

Fig. 3 presents the nanoscale morphologies of various block copolymer blend films assembled on the chemically patterned substrates. Single or multiple arrays of vertical cylinders were assembled along the underlying surface patterns (Fig. 3a–c). The schematic illustration of the assembled morphology (Fig. 3e) describes that the linear registry of vertical cylinder array is enforced by the surface parallel cylinders assembled along the PMMA preferential stripes of the surface pattern.[31] Between two neighboring surface parallel cylinders, vertical cylinder arrays were assembled along the neutral part of surface pattern. Despite the high energy penalty arising from the non-parallel arrangement of cylinders, this morphology consisting of an alternate vertical cylinder array and parallel cylinder is the equilibrium morphology for the cylinder forming block copolymers assembled on asymmetric neutral/preferential stripe patterns.[31] In this thin film morphology, the orientation of cylinders was dominantly determined by block copolymer film-substrate interfacial energy such that surface perpendicular cylinder arrays were assembled along the neutral stripe of surface pattern, while the surface parallel cylinder was assembled along the PMMA preferential stripe of the surface pattern. In the plane view SEM images, a weak trace of the single surface parallel cylinder is

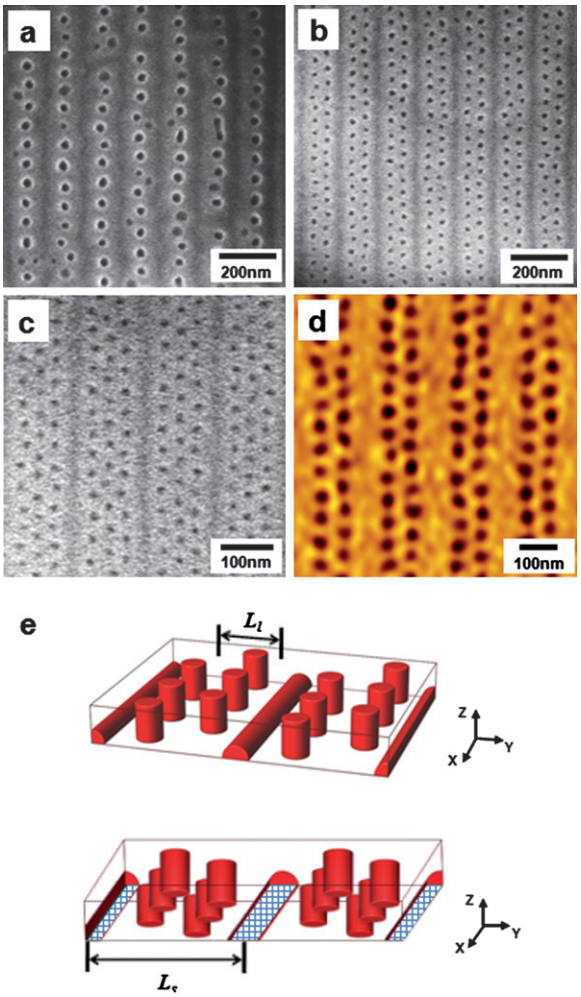

Fig. 3 (a)–(c) Plane view SEM images of multiple patterned block copolymer blend films assembled along chemically stripe patterned surfaces (143 nm pitch). (a) Single, (b) double, and (c) triple arrays of vertical cylinders were assembled as the cylinder layer period decreased with a blend composition (see Table 1). Note that the AFM image shown in (d) does not show any trace of surface parallel cylinders assembled at the bottom of the blend film. (e) A schematic illustration of double cylinder array morphology. The cross-hatched and transparent parts of the bottom surface correspond to polar and neutral surfaces, respectively.

observed between the vertical cylinder arrays. In contrast, the AFM image, shown in Fig. 3d, does not exhibit any trace of the surface parallel cylinder at the top surface of the block copolymer film (see ESI,† Fig. S2). This directed assembly of block copolymers into a complex morphology composed of orthogonally arranged cylinders enables the facile production of linear arrays of sub-20 nm-scale nanoholes or nanoposts, which are generally considered extremely challenging to produce by means of conventional ArF lithography.

The ordering of the multiple patterned morphology was crucially dependent upon the ratio of the underlying surface chemical pattern period (L_s) to the cylinder layer spacing of block copolymer blends (L_l). As noted in Table 1, a highly ordered double or triple cylinder array was created provided that L_s/L_l was 3.09 or 3.93, respectively, which is close to the integer value of 3 or 4. In contrast, the poorly ordered single layer

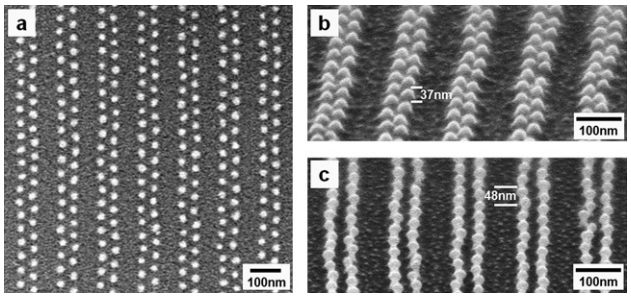

Fig. 4 SEM images of double arrays of Al nanodots and silica nanopillars templating a multiple patterned block copolymer blend film morphology. (a) Plane view of an Al dot array prepared by selective deposition through a nanoporous PS template and lift-off. Tilted views of (b) 37 nm-tall and (c) 48 nm-tall silica pillar arrays prepared by CF_4 RIE with an Al mask.

cylinder array had a non-integer L_s/L_l value of 2.35. Further optimization of the widths of the neutral and oxidized stripes of the surface pattern and its commensurability with the cylinder layer spacing of the block copolymer self-assembled morphology is anticipated to promote the defect-free ordering of various multiple patterned morphologies.

The block copolymer multiple patterned morphology could be replicated into a linear metal nanodot or silica nanopillar array by selective deposition or selective etching.[32,33] Firstly, a multiple patterned block copolymer thin film was exposed to UV radiation to selectively degrade the PMMA cylinders and crosslink the PS matrix. The degraded PMMA cylinders were completely removed by O_2 plasma etching. The remaining nanoporous PS layer was used as a deposition mask. Fig. 4a shows the double array of aluminium (Al) nanodots prepared by selective deposition of 10 nm Al through a PS mask and the subsequent lift-off. A well-ordered double array of Al nanodots that exactly replicated the double cylinder array morphology in a block copolymer thin film was produced over a large area (see ESI,† Fig. S3). The average diameter of metal nanodots and their neighboring center-to-center distance were 26 and 54 nm, respectively. Interestingly, the surface parallel cylinder morphology assembled at the bottom of the block copolymer film did not leave any trace in the pattern-transferred morphology. The metal nanodot array could be further utilized as an etching mask for the underlying silica ARC layer. Fig. 4b and 4c show the double array of silica nanopillars prepared by CF_4 RIE. Al metal dots successfully played the role of an etching mask such that a double array of silica pillars whose average height ranged from 30 to 50 nm could be created over a large area.

Conclusions

By integrating block copolymer assembly into a resolution enhancement technique for conventional ArF lithography, highly ordered linear arrays of a sub-20 nm scale cylinder morphology could be created, and subsequently pattern-transferred into a nanodot or nanopillar array. We anticipate that further engineering of this approach for diverse pattern shapes and dimensions would afford various nanopatterned components for memory[34] and photonic[35] devices by means of conventional ArF lithography. Moreover, further scaling down of this approach by employing the block copolymers with smaller self-assembled pattern dimensions[36] and advanced photolithography, such as immersion lithography and EUV projection lithography, would contribute to the continued shrinkage of critical device dimensions.

Acknowledgements

This work was financially supported by the second stage of the Brain Korea 21 Project, the National Research Laboratory Program (R0A-2008-000-20057-0), the Engineering Research Center (R11-2008-058-03002-0), KAIST EEWS initiatives (EEWS0903) and the Fundamental R&D Program for Core Technology of Materials funded by the Korean government (MEST, MKE).

Notes and references

1 International Technology Roadmap for Semiconductors, 2007 (www.itrs.net).
2 T. Skotnicki, J. A. Hutchby, T. J. King, H. S. P. Wong and F. Beouff, *IEEE Circuits Devices Mag.*, 2005, **21**, 16.
3 C. G. Willson and B. J. Roman, *ACS Nano*, 2008, **2**, 1323.
4 S. Hsu, J. Park, D. Van Den Broeke and J. F. Chen, *Proc. SPIE-Int. Soc. Eng.*, 2005, **5992**, 59921Q1.
5 M. Maenhoudt, J. Versluijs, H. Struyf, J. Van Olmen and M. Van Hove, *Proc. SPIE–Int. Soc. Opt. Eng.*, 2004, **5754**, 1508.
6 J. Park, S. Hsu, D. Van Den Broeke, J. F. Chen, M. Dusa, R. Socha, J. Finders, B. Vleeming, A. Van Oosten, P. Nikolsky, V. Wiaux, E. Hendrickx, J. Bekaert and G. Vandenberghe, *Proc. SPIE-Int. Soc. Eng.*, 2006, **6349**, 634922.
7 D. Y. Lee, Y. J. Chun, J. B. Yoon, S. H. Lee, S. J. Lee, H. K. Cho and J. T. Moon, *J. Vac. Sci. Technol., B*, 2006, **24**, 3105.
8 F. S. Bates and G. H. Fredrickson, *Phys. Today*, 1999, **52**, 32.
9 F. S. Bates and G. H. Fredrickson, *Annu. Rev. Phys. Chem.*, 1990, **41**, 525.
10 M. Park, C. Harrison, P. M. Chaikin, R. A. Register and D. H. Adamson, *Science*, 1997, **276**, 1401.
11 T. Thurn-Albrecht, J. Schotter, G. A. Kastle, N. Emley, T. Shibauchi, L. Krusin-Elbaum, K. Guarini, C. T. Black, M. T. Tuominen and T. P. Russell, *Science*, 2000, **290**, 2126.
12 S. O. Kim, H. H. Solak, M. P. Stoykovich, N. J. Ferrier, J. J. de Pablo and P. F. Nealey, *Nature*, 2003, **424**, 411.
13 R. Ruiz, H. Kang, F. A. Detcheverry, E. Dobisz, D. S. Kercher, T. R. Albrecht, J. J. de Pablo and P. F. Nealey, *Science*, 2008, **321**, 936.
14 I. Bita, J. K. W. Yang, Y. S. Jung, C. A. Ross, E. L. Thomas and K. K. Berggren, *Science*, 2008, **321**, 939.
15 S.-J. Jeong, J. E. Kim, H.-S. Moon, B. H. Kim, S. M. Kim, J.-B. Kim and S. O. Kim, *Nano Lett.*, 2009, **9**, 2300.
16 C. Tang, E. M. Lennon, G. H. Fredrickson, E. J. Kramer and C. J. Hawker, *Science*, 2008, **322**, 429.
17 K. Naito, H. Hieda, M. Sakurai, Y. Kamata and K. Asakawa, *IEEE Trans. Magn.*, 2002, **38**, 1949.
18 C. T. Black, K. W. Guarini, K. R. Milkove, S. M. Baker, T. P. Russell and M. T. Tuominen, *Appl. Phys. Lett.*, 2001, **79**, 409.
19 C. T. Black, K. W. Guarini, Y. Zhang, H. J. Kim, J. Benedict, E. Sikorski, I. V. Babich and K. R. Milkove, *IEEE Electron Device Lett.*, 2004, **25**, 622.
20 J. Y. Cheng, C. A. Ross, V. Z. H. Chan, E. L. Thomas, R. G. H. Lammertink and G. J. Vancso, *Adv. Mater.*, 2001, **13**, 1174.
21 D. H. Lee, D. O. Shin, W. J. Lee and S. O. Kim, *Adv. Mater.*, 2008, **20**, 2480.
22 D. H. Lee, W. J. Lee and S. O. Kim, *Nano Lett.*, 2009, **9**, 1427.
23 S.-J. Jeong, G. Xia, B. H. Kim, D. O. Shin, S.-W. Kang and S. O. Kim, *Adv. Mater.*, 2008, **20**, 1898.
24 Y. S. Jung, W. J. Jung and C. A. Ross, *Nano Lett.*, 2008, **8**, 2975.
25 C. T. Black, R. Ruiz, G. Breyta, J. Y. Cheng, M. E. Colburn, K. W. Guarini, H.-C. Kim and Y. Zhang, *IBM J. Res. Develop.*, 2007, **51**, 605.
26 C. T. Black, *ACS Nano*, 2007, **1**, 147.

27 P. Mansky, Y. Liu, E. Huang, T. P. Russell and C. Hawker, *Science*, 1997, **275**, 1458.
28 M. P. Stoykovich, M. Muller, S. O. Kim, H. H. Solak, E. W. Edwards, J. J. de Pablo and P. F. Nealey, *Science*, 2005, **308**, 1442.
29 T. Shibata, S. Nakagawa, Y. Sato, K. Sho, H. Hayashi and J. Abe, *Proc. SPIE–Int. Soc. Opt. Eng.*, 2002, **4690**, 773.
30 Y. Kang, S.-G. Woo, S.-J. Choi and J.-T. Moon, *Proc. SPIE–Int. Soc. Opt. Eng.*, 2001, **4345**, 222.
31 S. O. Kim, B. H. Kim, D. Meng, D. O. Shin, C. M. Koo, H. H. Solak and Q. Wang, *Adv. Mater.*, 2007, **19**, 3271.
32 D. Zschech, D. H. Kim, A. P. Milenin, R. Scholz, R. Hillebrand, C. J. Hawker, T. P. Russell, M. Steinhart and U. Gösele, *Nano Lett.*, 2007, **7**, 1516.
33 K. W. Guarini, C. T. Black, Y. Zhang, H. Kim, E. M. Sikorski and I. V. J. Babich, *J. Vac. Sci. Technol., B*, 2002, **20**, 2788.
34 C. A. Ross, *Annu. Rev. Mater. Res.*, 2001, **31**, 203.
35 S. A. Maier, P. G. Kik, H. A. Atwater, S. Meltzer, E. Harel, B. E. Koel and A. A. G. Requicha, *Nat. Mater.*, 2003, **2**, 229.
36 S. Park, D. H. Lee, B. Kim, S. W. Hong, U. Jeong, T. Xu and T. P. Russell, *Science*, 2009, **323**, 1030.